AIMS Materials Science, 8(4): 524–537.
DOI: 10.3934/matersci.2021032
Received: 15 April 2021
Accepted: 03 June 2021
Published: 24 June 2021

http://www.aimspress.com/journal/Materials

Research article

Exploring the possibilities of FDM filaments comprising natural fiber-reinforced biocomposites for additive manufacturing

Mahdi Rafiee[1], Roozbeh Abidnejad[1], Anton Ranta[1], Krishna Ojha[1], Alp Karakoç[1,2,*], and Jouni Paltakari[1]

[1] Aalto University, Department of Bioproducts and Biosystems, Vuorimiehentie 1, Espoo, Finland
[2] Aalto University, Department of Communications and Networking, Maarintie 8, Espoo, Finland

* **Correspondence:** Email: alp.karakoc@alumni.aalto.fi; Tel: +358503442937.

Abstract: In recent years, with the recent advancements in the field of additive manufacturing, the use of biobased thermoplastic polymers and their natural fiber-reinforced biocomposite filaments have been rapidly emerging. Compared to their oil-based counterparts, they provide several advantages with their low carbon footprints, ease of reusability and recyclability and abundancy, and comparable price ranges. In consideration of their increasing usage, the present study focused on the development and analysis of biocomposite material blends and filaments by merging state-of-the-art manufacturing and material technologies. A thorough suitability study for fused deposition modeling (FDM), which is used to manufacture samples by depositing the melt layer-by-layer, was carried out. The mechanical, thermal, and microstructural characterization of birch fiber reinforced PLA composite granules, in-house extruded filaments, and printed specimens were investigated. The results demonstrated the printability of biocomposite filaments. However, it was also concluded that the parameters still need to be optimized for generic and flawless filament extrusion and printing processes. Thus, minimal labor and end-products with better strength and resolutions can be achieved.

Keywords: Additive manufacturing; 3D printing; fused deposition modelling (FDM); filament extrusion; biocomposites; recyclability

1. Introduction

The development of synthetic composites has allowed researchers to design lightweight yet

durable and robust structures, which are nowadays used widely in transportation, construction, biomedicine, and packaging industries [1–6]. However, in recent years, there is a growing interest towards biobased and biodegradable composites due to their renewability, CO_2 neutrality, and lower cost [7]. The utilization of biobased resources advances the independence from non-renewable fossil fuel resources, while biodegradability brings added value to the products by minimizing environmental pollution [8,9].

The most promising biobased reinforcements for composites are natural lignocellulosic fibers. Refinery of these fibers is a mature industrial technology, for which a lot of research effort has been made in order to utilize their strength for new applications [10]. Natural fibers are not up to par with synthetic fibers in absolute strength; however, their specific mechanical properties can compete with their counterparts. In addition to the lower strength, natural fiber reinforcements and plastic matrices are not inherently compatible due to their hydrophilic and hydrophobic nature, respectively. In order to enhance the performance of natural fiber reinforced polymer composites, numerous approaches have been developed in the literature. For instance, surface hydroxyl-groups in cellulose and natural fibers have been targeted as chemical modification substrate, polymer grafting of cellulose have been prepared, and physical treatments have been carried out in order to overcome the compatibility issues [11–13]. These approaches have aimed at enhancing the matrix-reinforcement interfacial adhesion, which is essential for successful stress transfer from matrix to reinforcement phase [14–16].

In addition to the fibers as reinforcement, the polymers as the matrix material play a critical role in composites. Since their discovery, the use of polymers was widespread in many different applications, including food packaging, clothing, construction, automotive, aviation, communication, to name a few [17,18]. They are the most produced oil-based products, which are mostly non-biodegradable and have potential danger for the environment. On the other hand, there exist biodegradable polymers that can be entirely degraded by the action of naturally occurring microorganisms such as bacteria, fungi, and algae [19,20]. This type of biobased polymers is produced from renewable carbon resources and is known to be environmentally friendly [21]. The waste disposal problems are hence less stressed out with the use of these polymers in comparison with the nondegradable polymers. However, similar to the natural lignocellulosic fibers, biobased and biodegradable polymers need to fulfill material and process-related criteria, including strength, non-toxicity, permeability, moisture resistance, high thermal properties, along with low-cost production and processing.

The methods for the production of biobased and biodegradable polymers are classified into three main groups based on both the processes involved and types of the polymers, which are (I) chemical polymerization of monomers derived from the biological process, (II) the direct biosynthesis of polymers in microorganisms and (III) modification of natural polymers [17]. Some examples of polymers produced by such methods are polylactic acid (PLA) (method I), polyhydroxyalkanoate (PHA) (method II), and starch, cellulose (method III). Out of these polymers, PLA is one of the most commonly used biobased polymers, which is produced from lactic acid and synthesized by microorganisms using glucose. Usually, the glucose is obtained from the corn starch and sugar cane as the carbon source via fermentation with lactic bacteria [22]. The monomers of PLA are enantiomeric, having L- and D-isomers which help to prepare amorphous to crystalline polymers possessing different physical, chemical, mechanical, and degradation properties [23]. It has been widely used in the industry, e.g., for packaging, drug delivery, medical implantations. However, pure

PLA is brittle, so its use is limited for most of these applications. Therefore, this is usually overcome by blending it with other polymers, which results in enhanced mechanical properties [24]. In recent years, advances in additive manufacturing (AM) technologies combined with the commodity thermoplastics set the ground for the use of PLA in both prototyping and large volume production [25–27]. Nevertheless, research studies have been carried out over AM and the effective use of thermoplastics and their composites towards developing reliable and repeatable processes [28–30]. Thus, conventional fabrication technologies with excessive waste material are aimed to be replaced [31,32]. However, a limited variety of environmentally friendly yet 3D printable materials are such an example of the development challenges as being a critical barrier to the widescale use of biobased 3D printing technologies. A vast number of investigations have been conducted on the development and use of such materials, especially with the fused deposition modeling (FDM) as a 3D printing process, which is based on filament softening and extrusion through a nozzle, as illustrated in Figure 1 [33]. The main reasons to use FDM as a research tool are its ease of accessibility and affordability [34–36]. In addition, a wide variety of thermoplastic polymers, including PLA, can also be used with FDM. However, it is also worth mentioning that maintaining an optimum melt flow viscosity at low temperatures for FDM has been challenging and under investigation. Two solutions to resolve this issue are favored in the literature, which are (I) increasing the temperature during processing and (II) the use of a suitable plasticizer [37]. The latter solution is more superior as it prevents thermal degradation [38].

As outlined in Figure 1a, the present study hence aims at overcoming the challenges in 3D filament extrusion/production and printing of natural fiber reinforced PLA biocomposites and enhancing their performance by blending the granules and polyethylene glycol (PEG) plasticizing agent to induce ductility and toughness while providing strength through the natural fibrous reinforcement. Various fiber and PEG weight fractions were investigated to understand the mechanical performance of their filaments and FDMed specimens. The effect of PEG and natural fiber loading on thermal properties was also studied by thermogravimetric analysis (TGA) and differential scanning calorimetry (DSC). The results demonstrated the printability of investigated materials; however, optimization of both extrusion and printing parameters should be carried out for a flawless and repeatable process.

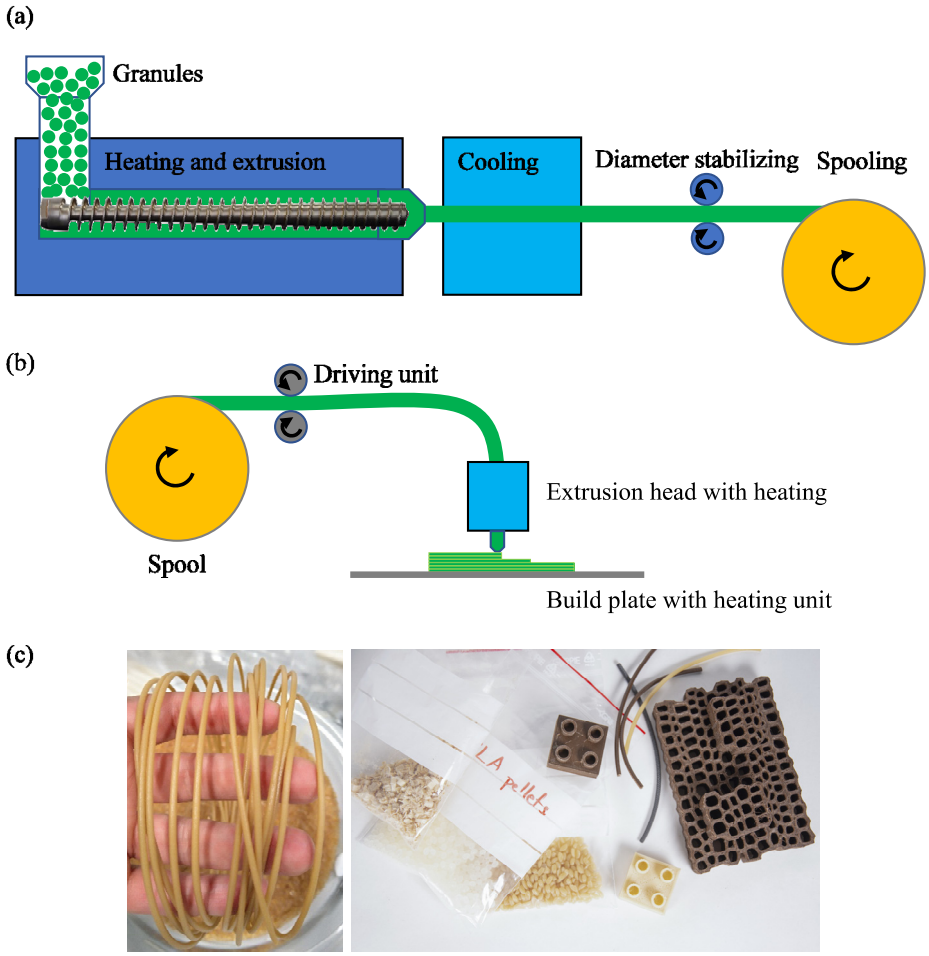

Figure 1. 3D filament production and printing workflow of the present study: (a) filament production, (b) illustration of fused deposition modeling (FDM) (reproduced from [36]), (c) raw materials, filaments, and some 3D printed samples with FDM (photo by Valeria Azovskaya).

2. Materials and methods

2.1. Thermoplastic polymer composite filaments and 3D printing

Granules of PLA/birch fiber blend and pure PLA (Ingeo biobased PLA3251D) were used as provided by the client. In order to reduce the hydrophobicity, increase the surface energy of the matrix and improve the wetting on the fiber surface, PEG flakes with 2000 Da molecular weight (Merck, Germany) were used as the plasticizer [39]. Prior to filament preparation, PLA/birch fiber granules were vacuum dried overnight at 60 °C. After drying, the appropriate amount of PEG was tumble mixed with the PLA/birch fiber granules to obtain approximately 300 g batch. Each batch was separately prepared into a filament with a 3devo Composer 450 desktop filament maker (Utrecht, Netherlands). The operator of the filament maker varied three parameters manually in order to obtain consistent filament: screw speed, the temperature of the screw chamber, spooling speed. The initial extrudate was discarded until the consistency of the extrudate was considered consistent. The cooling

procedure of filaments, as seen in Figure 1a, was carried out by a dual-fan system, which provides even air distribution, installed on the left and right sides of the nozzle. The fan's speed was adjusted to 100%, and their angle was modified for the maximum quality output. Each batch was processed into 1.75 mm filament in diameter for 3D printing, the compositions of which are listed in Table 1.

Table 1. Filament composition and sample coding. PLA and birch fiber fractions refer to the granule's composition, while PEG fractions were calculated based on the dry mass of the granules prepared for filament production.

Sample coding	PLA (wt% of the granules)	Birch fiber (wt% of the granules)	PEG (wt% of the material dry mass added to filament maker)
PLA0%-PEG0%	100	0	0
PLA0%-PEG1%	100	0	1
PLA0%-PEG5%	100	0	5
PLA0%-PEG10%	100	0	10
PLA1%-PEG0%	99	1	0
PLA1%-PEG1%	99	1	1
PLA1%-PEG5%	99	1	5
PLA1%-PEG10%	99	1	10
PLA5%-PEG0%	95	5	0
PLA5%-PEG1%	95	5	1
PLA5%-PEG5%	95	5	5
PLA5%-PEG10%	95	5	10
PLA10%-PEG0%	90	10	0
PLA10%-PEG1%	90	10	1
PLA10%-PEG5%	90	10	5
PLA10%-PEG10%	90	10	10

The manufactured filaments were then used to print tensile testing specimens with Wanhao i3 Plus Duplicator 3D printer as an affordable choice having both the extrusion motor and injector at the same place. As shown in Figure 2, the tensile testing specimens were prepared according to ISO 527-1:2012. The infill was 100% with a diagonal grid pattern with respect to the longitudinal axis. Samples were made using 100 % injection speed (material flow), 210 ^{o}C hot-end temperature, 100% fan speed, 70 ^{o}C bed temperature, and 40 mm/s printing speed.

2.2. Scanning electron microscopy (SEM)

The morphology of the granules, filaments, and cross-sections of the tensile testing specimens was investigated by a field emission scanning electron microscopy (Zeiss Sigma VP, Germany) using an acceleration voltage of 1.5 kV. Prior to capturing images, samples were coated with a 5 nm gold/palladium layer by Leica EM ACE600 high vacuum sputter coater.

2.3. Thermogravimetric analysis (TGA) and differential scanning calorimetry (DSC)

The thermal stability of each material was studied with a linear temperature ramp protocol using

TGA analysis. The crystallization and melting transition behavior of the materials were investigated by the DSC. The samples obtained after producing filament form PLA/birch fiber granules mixed with PEG at different percent ratios were analyzed using Netsch STA 449 F3 Jupiter for thermal characterization. The DSC and TGA were performed in parallel with the samples of mass around 10 mg, which were then heated up to 500 °C at 10 °C/min under a helium atmosphere. The helium was purged continuously at a flow rate of 50 mL/min.

2.4. Mechanical characterization

Each series was conditioned in the tensile testing facilities for one week in order to obtain reproducibility of the process due to the hygroscopic nature of the prepared materials [42]. Tensile testing was performed with Zwick MTS 1475 universal material testing machine in 60% relative humidity and 23 °C using a 1mm/min strain rate and 100 mm gauge length. The instrument software was used to record the stress, strain, energy to peak, and tensile strength. The average and standard deviation of each key figure for each series were then calculated by the lab operator.

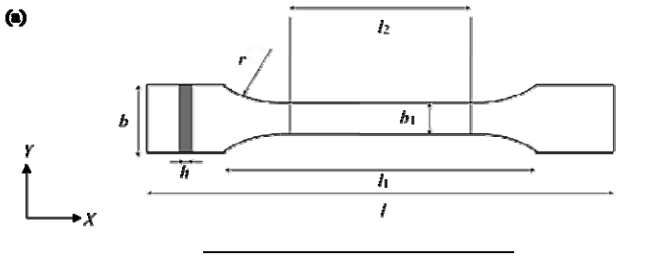

Details	Dimension (mm)
Full length, l	170
Grip face length, l_1	112
Parallel test length, l_2	80
Grip section width, b_2	20
Parallel section width, b_1	10
Thickness, h	4
Radius, r	20

Figure 2. 3D printed specimens: (a) dimensional specifications according to ISO 527-1:2012 [40,41], (b) printed specimen with the Wanhao i3 Plus Duplicator 3D printer.

3. Results and discussion

3.1. Morphology

Figure 3 depicts the representative SEM images for the granules and the damage zones of the tensile specimens. Figure 3a demonstrated the existence of significant gaps between the layers of the

tensile specimens, which is assumed to be a combined artifact of the filament quality and material flow during the printing process. The red arrows in these figures show the most prominent gaps impairing the print quality and causing non-homogeneities in the microstructure. In contrast to what had been expected, the addition of PEG to the system (please, see Figure 3b) resulted in further incompatibility inside the composites and resulted in small voids. On the other hand, ruptured fibers within the polymer matrix were captured at the cross-section of the tensile damage zone in Figure 3c,d. According to the fiber morphology and the bonding with the matrix, it was concluded that fibers pull-out was the dominant damage mechanism during the tensile testing. This indicates the weak bonding at the fiber-matrix interface. It is also noteworthy that the fibers were more apparent in the granules, as seen in Figure 3e. Considering the presence of fibers inside the granules, filament making or printing process (or both) were deduced to have a negative impact on the homogenous structure of fiber and polymer.

As indicated with red circles in Figure 3e,f, two types of voids were observed, where the first type was in the form of small holes inside the granule while the latter was in the form of large holes located in the center of the granule as shown in Figure 3f. None of these void types were observed in the neat PLA, which means that each granule (except neat PLA) is in the form of a hollow sphere lacking the right amount of infill. This is assumed to be due to the trapped air during the granule production and affected the filament-making process unfavorably.

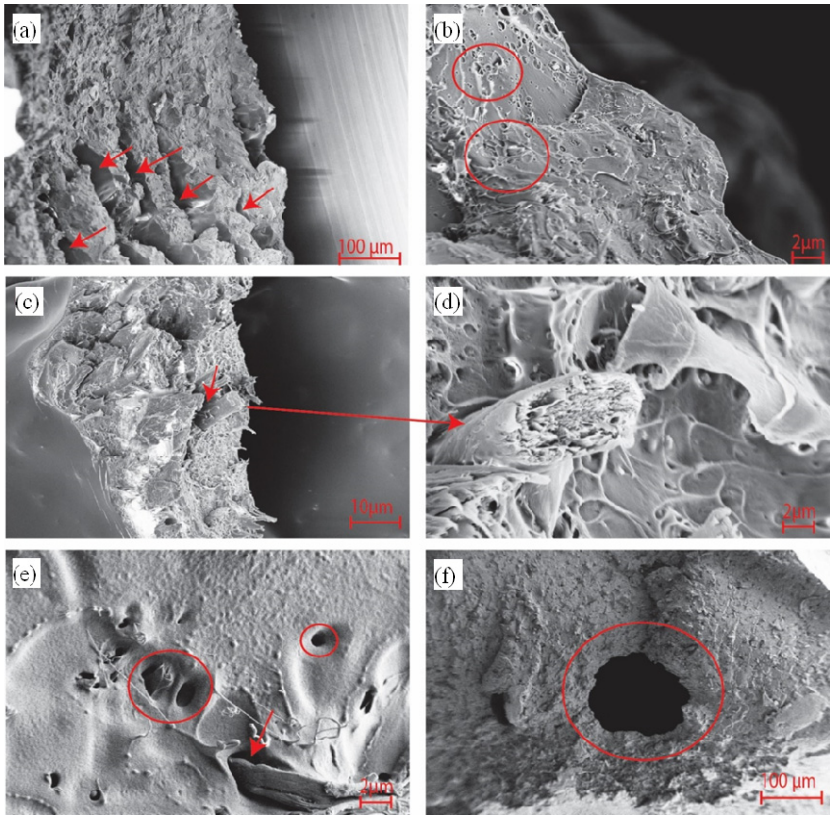

Figure 3. SEM pictures captured from tensile samples cross section and initial granules. (a) PLA10%-PEG0%, (b) PLA10%-PEG10%, (c–d) PLA10%-PEG1%, (e) PLA5% granule and (f) PLA10% granule. Red arrows and circles indicate fiber reinforcement and void, respectively.

3.2. Tensile testing

The key figures of mechanical performance for each material are presented in Table S1 as Supplementary, while representative stress-strain curves for each material are illustrated in Figure 4. Tested specimens were determined to be brittle with a negligible plasticization effect despite the addition of PEG. It was beheld that introducing fibers into PLA reduced elongation to peak and energy (of fracture) to the peak. Despite the expected positive influence, Young's modulus and tensile strength decreased with the increasing fiber content up to 10 weight percent (wt%) of fiber. In comparison, 20 wt% fiber loading demonstrated an increase in tensile strength and modulus. Similar observations have been made in the literature by Masirek and his colleagues, who studied the effect of hemp fiber in PLA/PEG blends [43]. As a similar trend, increasing fiber weight percentages in neat PLA resulted in decreasing Young's Modulus. This indicates that the applied stress is not transferred from the matrix to the fibers due to poor interfacial adhesion. Furthermore, it was also deduced that the mixing efficiency of the filament maker was not sufficient to process polymer blends or composites. The authors suggest that a more thorough mixing of components ought to be performed before filament preparation.

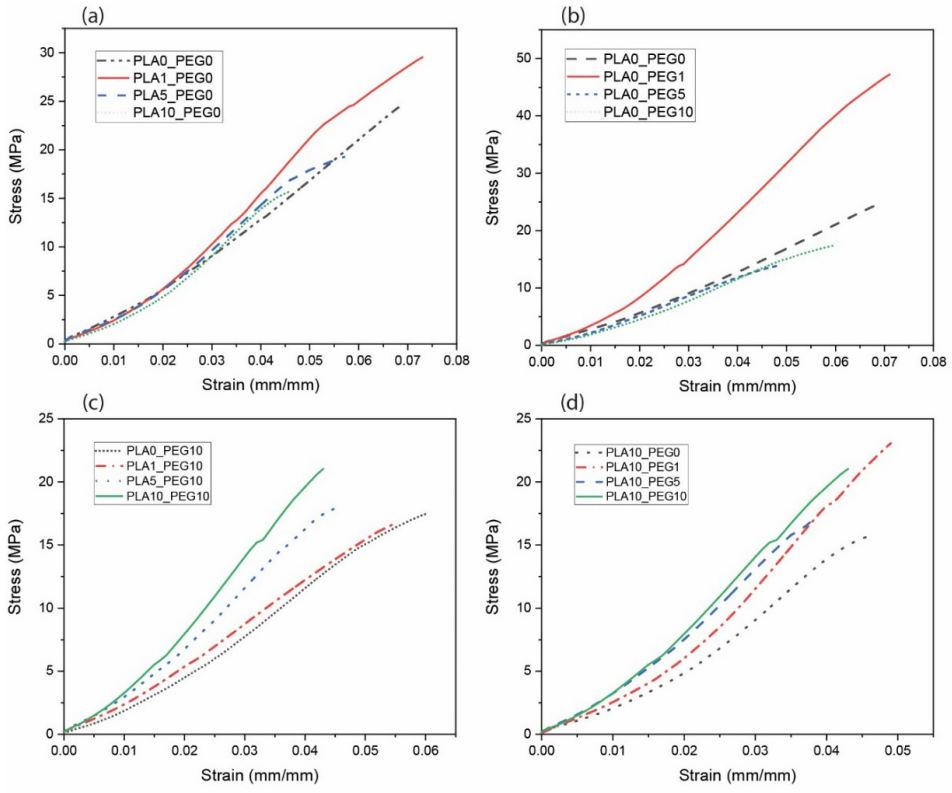

Figure 4. Stress-strain curves for: (a) without PEG, (b) without fiber reinforcement, (c) maximum amount of PEG used, (d) maximum amount of fiber reinforcement.

Additional to the stress-strain results, the average ultimate tensile strength was calculated to have a better understanding of mechanical properties. The overview of the results in Figure 5 illustrates three categories, where the first and second categories were highlighted with the red and

blue dots, respectively. The rest was considered as the third domain without any marks. First and foremost, it is clear that in contrast to the a priori expectation, neat PLA samples showed the highest mechanical strength (red circles). The difference between these samples and the rest was significant. Moreover, considering the fact that compatibilization plays a vital role in composites, the outcome of SEM and ultimate tensile strength shed light on the fact that the compatibilization of components (PLA, fiber, and PEG) during the filament making process was carried out poorly. On the other hand, samples with the highest PEG fraction and low fiber fraction (samples 4 and 8 of Figure 5) resulted in the lowest ultimate tensile strength values. However, by increasing the fiber fraction (samples 12 and 16 of Figure 5), the mechanical properties were slightly improved. Applying large amounts of PEG and fiber reinforcement hence indicated higher packing between the fiber network but less efficient cross-linking of PLA-fiber-PEG. In the case of the second category (blue circles), specifically samples 5, 6, and 7 of Figure 5, it can be observed that the second-highest mechanical values still belong to low fiber fractions, which supports the earlier statements. No clear interaction between the fibers and PEG was obtained. However, it is clear that the fiber as reinforcement for polymeric matrix and PEG as a well-known plasticizer did not play their performance-enhancing role due to the voids in the granules and artifacts in both filament extrusion and printing processes.

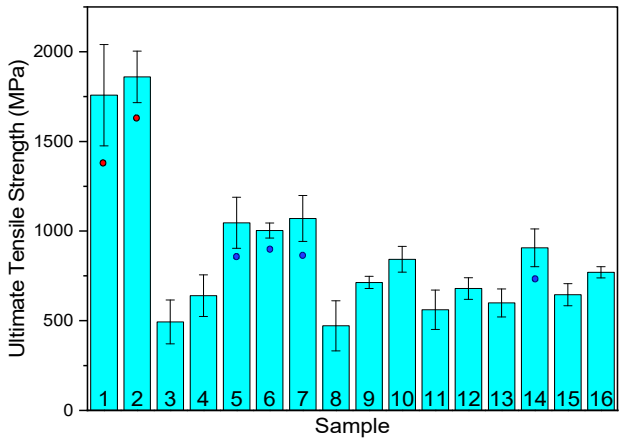

Figure 5. Mean values of ultimate tensile strength for all samples: (1) PLA0%-PEG0%, (2) PLA0%-PEG1%, (3) PLA0%-PEG5%, (4) PLA0%-PEG10%, (5) PLA1%-PEG0%, (6) PLA1%-PEG1%, (7) PLA1%-PEG5%, (8) PLA1%-PEG10%, (9) PLA5%-PEG0%, (10) PLA5%-PEG1%, (11) PLA5%-PEG5%, (12) PLA5%-PEG10%, (13) PLA10%-PEG0%, (14) PLA10%-PEG1%, (15) PLA10%-PEG5%, (16) PLA10%-PEG10%.

3.3. Thermogravimetric analysis (TGA) and Differential Scanning Calorimetry (DSC)

As the first step in the TGA, the moisture was removed by heating the samples. During this step, initial changes in the mass were observed. The onset value of TGA at the later stage was found to be in the range of 318–354 °C, as illustrated in Figures 6 and 7 and tabulated in Table S2 as Supplementary. There have been some changes in the degradation temperature by the addition of PEG. However, the differences were not drastic and dependent on any parameter despite similar conditions. Previous studies suggest that the onset TGA value ranges from 338–376 °C for biobased

pure PLA [44]. This indicates that birch fiber reinforcement plays a role in decreasing the degradation temperature. The final degradation took place beyond 350 °C, where 95% to 100% of the material was decomposed. Kakuta et al. and Yang et al. mentioned in their work the melting temperature (Tm) of the biobased PLA as 160–170 °C [23,44]. Whereas our samples were composed of birch fiber reinforced PLA along with PEG, and the Tm ranged from 160.2–172.9 °C. This indicates that birch fibers and the PEG blend do not affect the thermal properties of the extruded filaments.

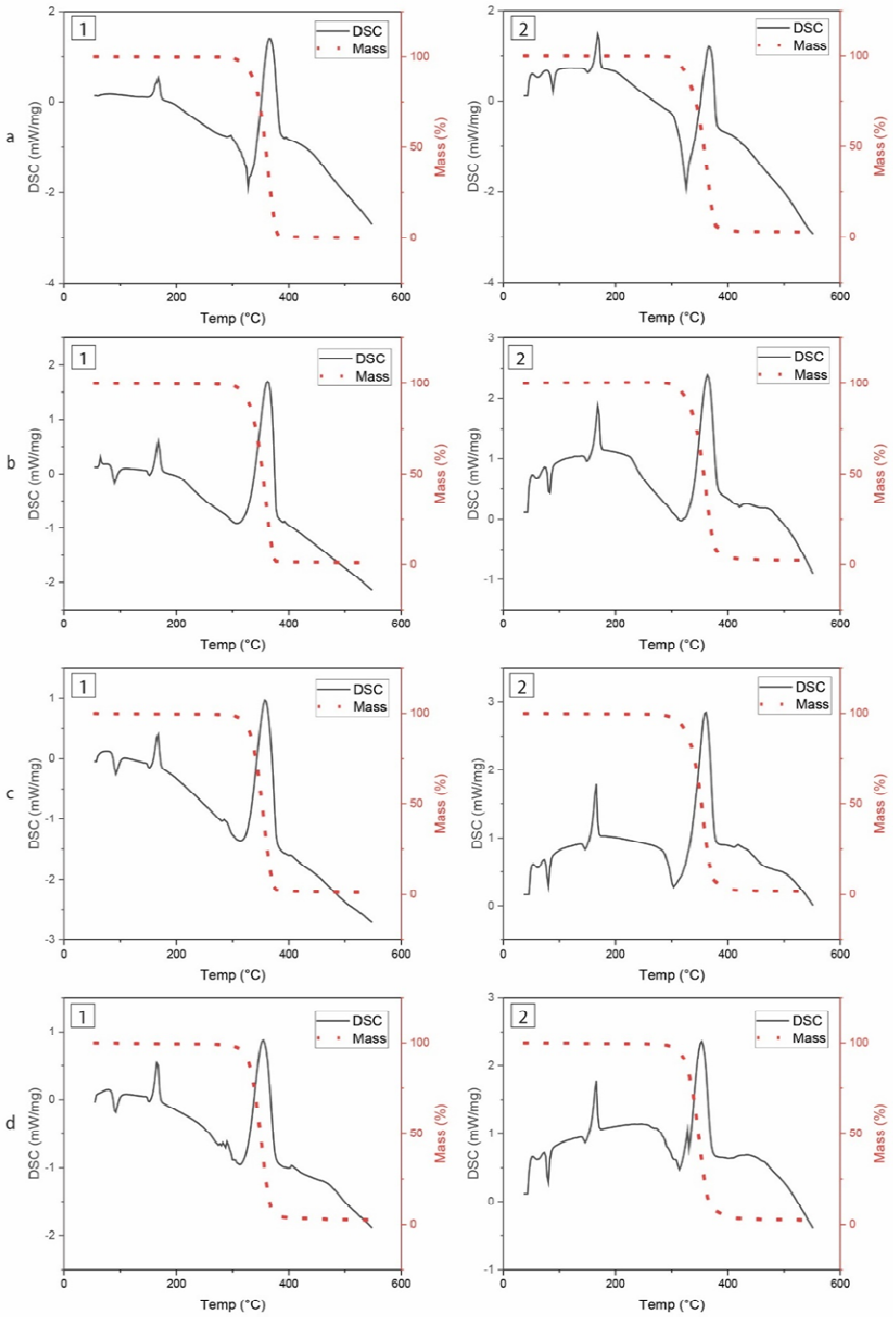

Figure 6. Results of TGA/DSC as a function of temperature: (a) PLA 0%, (b) PLA 1%, (c) PLA 5% and (d) PLA 10%. Here, 1 represents the PLA granule and 0% PEG, 2 represents PLA filament with 10% PEG.

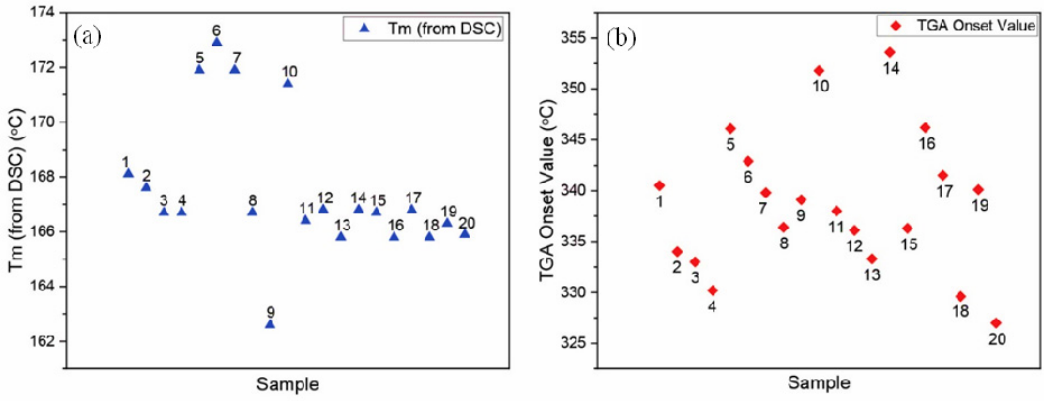

Figure 7. Illustration of (a) melting point (Tm) and (b) TGA onset values for all samples. Labels 1–16 represent the filaments and labels 17–20 stand for the granules. To elaborate, (1) PLA0%-PEG0%, (2) PLA0%-PEG1%, (3) PLA0%-PEG5%, (4) PLA0%-PEG10%, (5) PLA1%-PEG0%, (6) PLA1%-PEG1%, (7) PLA1%-PEG5%, (8) PLA1%-PEG10%, (9) PLA5%-PEG0%, (10) PLA5%-PEG1%, (11) PLA5%-PEG5%, (12) PLA5%-PEG10%, (13) PLA10%-PEG0%, (14) PLA10%-PEG1%, (15) PLA10%-PEG5%, (16) PLA10%-PEG10%, (17) PLA0%, (18) PLA1%, (19) PLA5% and (20) PLA10%.

4. Conclusions

Based on the investigations and presented results for filament fabrication and 3D printing based on FDM, the desktop filament maker in use was obtained to be not working as efficiently as expected. One of the main reasons for the extruder performance was the length of the extrusion screw, which resulted in short time spans for blending, clogging, and diameter variations in the extruded filament. As a result of these flaws, the filament-making process had a large amount of residue, which in turn caused an increase in raw material consumption. In order to solve this problem, it is suggested that an improved extrusion and blending system prior to the filament maker (which is crucial for the diameter of the filament) would be beneficial for a more homogeneous blend of polymer/fiber/PEG, which was also emphasized in very recent publications [45,46].

Furthermore, during the 3D printing process, several challenging issues existed. First and foremost, the printing parameters, including nozzle and print-bed temperatures and material flow rate, were difficult to be optimized for the investigated filaments. The fabrication of specimens by printing was a time-consuming process, e.g., 3D printing of each tensile sample (combined with errors at the start, during printing, and after finishing) took 3-4 hours while it could take up to seconds-to-minutes for injection molding once the process parameters are optimized. Moreover, another challenge of the 3D printing process was the brittle nature of the filaments, which caused filament breakage and clogging inside the nozzle system of the printer. This flaw limited the range of 3D printers that can be used during this project. In other words, the printers having both the extrusion motor and nozzle at the same place produce more reliable and repeatable results with such filaments. However, removing the broken filaments from such a mechanism required complete disassembling of the printer head apart, which was also time-consuming and not desired. Overall, the printing quality was not as expected with this process as there existed inconsistency and high standard deviation in the

mechanical testing results. The authors suggest a more thorough investigation on the blending of the components and printing process parameter optimization to overcome these issues for repeatable and reliable process development.

Acknowledgments

The authors would like to acknowledge the material support by Elastopoli Oy, Finland. Both M.R. and R.A. had equal contributions; therefore, their co-authorship order should be equally assessed. A.K. gratefully acknowledges the funding through the Academy of Finland BESIMAL (Decision No. 334197).

Conflict of interests

The authors declare no conflict of interest.

References

1. Parandoush P, Lin D (2017) A review on additive manufacturing of polymer-fiber composites. *Compos Struct* 182: 36–53.
2. Gopinathan J, Noh I (2018) Recent trends in bioinks for 3D printing. *Biomater Res* 22: 1–15.
3. Rahim TNAT, Abdullah AM, Md Akil H (2019) Recent developments in fused deposition modeling-based 3D printing of polymers and their composites. *Polym Rev* 59: 589–624.
4. Karakoç A (2017) A brief review on sustainability criteria for building materials. *Juniper Online J Mater Sci* 2: 1–3.
5. Shahrubudin N, Lee TC, Ramlan R (2019) An overview on 3D printing technology: Technological, materials, and applications. *Procedia Manuf* 35: 1286–1296.
6. Campbell T, Williams C, Ivanova O, et al. (2011) Could 3D printing change the world?: Technologies, potential, and implications of additive manufacturing. Washington, DC: Atlantic Council, 3.
7. Dou J, Karakoç A, Johansson LS, et al. (2021) Mild alkaline separation of fiber bundles from eucalyptus bark and their composites with cellulose acetate butyrate. *Ind Crop Prod* 165: 113436.
8. Faruk O, Bledzki AK, Fink HP, et al. (2012) Biocomposites reinforced with natural fibers: 2000–2010. *Prog Polym Sci* 37: 1552–1596.
9. Karakoc A, Bulota M, Hummel M, et al. (2021) Effect of single-fiber properties and fiber volume fraction on the mechanical properties of Ioncell fiber composites. *J Reinf Plast Compos* 0: 1–8.
10. Sixta H, Michud A, Hauru L, et al. (2015) Ioncell-F: A high-strength regenerated cellulose fibre. *Nord Pulp Pap Res J* 30: 43–57.
11. Li X, Tabil LG, Panigrahi S (2007) Chemical treatments of natural fiber for use in natural fiber-reinforced composites: A review. *J Polym Environ* 15: 25–33.
12. Wei L, McDonald AG (2016) A review on grafting of biofibers for biocomposites. *Materials* 9: 303.

13. Kalia S, Kaith BS, Kaur I (2009) Pretreatments of natural fibers and their application as reinforcing material in polymer composites-a review. *Polym Eng Sci* 49: 1253–1272.
14. Hayward MR, Johnston JH, Dougherty T, et al. (2019) Interfacial adhesion: improving the mechanical properties of silicon nitride fibre-epoxy polymer composites. *Compos Interface* 26: 263–273.
15. Nogueira CL, De Paiva JMF, Rezende MC (2005) Effect of the interfacial adhesion on the tensile and impact properties of carbon fiber reinforced polypropylene matrices. *Mater Res* 8: 81–89.
16. Wong KH, Syed Mohammed D, Pickering SJ, et al. (2012) Effect of coupling agents on reinforcing potential of recycled carbon fibre for polypropylene composite. *Compos Sci Technol* 72: 835–844.
17. Sudesh K, Iwata T (2008) Sustainability of biobased and biodegradable plastics. *Clean-Soil Air Water* 36: 433–442
18. Wohlers T (2017) Additive manufacturing and composites: An update. *Compos World* 3: 6.
19. Vroman I, Tighzert L (2009) Biodegradable polymers. *Materials* 2: 307–344.
20. Pandey JK, Pratheep Kumar A, Misra M, et al. (2005) Recent advances in biodegradable nanocomposites. *J Nanosci Nanotechno* 5: 497–526.
21. Iwata T (2015) Biodegradable and biobased polymers: Future prospects of eco-friendly plastics. *Angew Chemie Int Edit* 54: 3210–3215.
22. Farah S, Anderson DG, Langer R (2016) Physical and mechanical properties of PLA, and their functions in widespread applications—A comprehensive review. *Adv Drug Deliver Rev* 107: 367–392.
23. Kakuta M, Hirata M, Kimura Y (2009) Stereoblock polylactides as high-performance biobased polymers. *J Macromol Sci* 49: 107–140.
24. Garrison TF, Murawski A, Quirino RL (2016) Biobased polymers with potential for biodegradability. *Polymers* 8: 262.
25. Senatov FS, Niaza KV, Zadorozhnyy MY, et al. (2016) Mechanical properties and shape memory effect of 3D-printed PLA-based porous scaffolds. *J Mech Behav Biomed* 57: 139–148.
26. Bose S, Vahabzadeh S, Bandyopadhyay A (2013) Bone tissue engineering using 3D printing. *Mater Today* 16: 496–504.
27. Hutmacher DW, Schantz JT, Lam CXF, et al. (2007) State of the art and future directions of scaffold-based bone engineering from a biomaterials perspective. *J Tissue Eng Regen M* 1: 245–260.
28. Cicala G, Latteri A, Curto B Del, et al. (2017) Engineering thermoplastics for additive manufacturing: A critical perspective with experimental evidence to support functional applications. *J Appl Biomater Func* 15: 10–18.
29. Picard M, Mohanty AK, Misra M (2020) Recent advances in additive manufacturing of engineering thermoplastics: Challenges and opportunities. *RSC Adv* 10: 36058–36089.
30. Keleş Ö, Anderson EH, Huynh J, et al. (2018) Stochastic fracture of additively manufactured porous composites. *Sci Rep* 8: 1–12.
31. Blok LG, Longana ML, Yu H, et al. (2018) An investigation into 3D printing of fibre reinforced thermoplastic composites. *Addit Manuf* 22: 176–186.
32. Hausman KK, Horne R (2014) *3D Printing For Dummies*, John Wiley & Sons.

33. Wang X, Jiang M, Zhou Z, et al. (2017) 3D printing of polymer matrix composites: A review and prospective. *Compos Part B-Eng* 110: 442–458.
34. El Moumen A, Tarfaoui M, Lafdi K (2019) Modelling of the temperature and residual stress fields during 3D printing of polymer composites. *Int J Adv Manuf Tech* 104: 1661–1676.
35. Sajaniemi V, Karakoç A, Paltakari J (2019) Mechanical and thermal behavior of natural fiber-polymer composites without compatibilizers. *RESM* 6: 62–73.
36. Karakoç A, Rastogi VK, Isoaho T, et al. (2020) Comparative screening of the structural and thermomechanical properties of FDM filaments comprising thermoplastics loaded with cellulose, carbon and glass fibers. *Materials* 13: 422.
37. Kaynak C, Varsavas SD (2019) Performance comparison of the 3D-printed and injection-molded PLA and its elastomer blend and fiber composites. *J Thermoplast Compos* 32: 501–520.
38. Zhuang Y, Song W, Ning G, et al. (2017) 3D–printing of materials with anisotropic heat distribution using conductive polylactic acid composites. *Mater Design* 126: 135–140.
39. Li D, Jiang Y, Lv S, et al. (2018) Preparation of plasticized poly(lactic acid) and its influence on the properties of composite materials. *PLOS One* 13: e0193520.
40. Lafranche E, Oliveira VM, Martins CI, et al. (2015) Prediction of injection-moulded flax fibre reinforced polypropylene tensile properties through a micro-morphology analysis. *J Compos Mater* 49: 113–128.
41. International Organization for Standardization (2012) Plastics—Determination of tensile properties—Part 1: General principles, ISO 527-1: 2012.
42. Hua J, Zhao ZM, Yu W, et al. (2011) Mechanical properties and hygroscopicity of polylactic acid/wood-flour composite. *J Funct Mater* 42: 1762–1764+1767.
43. Masirek R, Kulinski Z, Chionna D, et al. (2007) Composites of poly(L-lactide) with hemp fibers: Morphology and thermal and mechanical properties. *J Appl Polym Sci* 105: 255–268.
44. Yang S, Madbouly SA, Schrader JA, et al. (2015) Characterization and biodegradation behavior of biobased poly(lactic acid) and soy protein blends for sustainable horticultural applications. *Green Chem* 17: 380–393.
45. Johnson D (2020) Filament extrusion using recycled materials: Experimental investigations on recycled Polylactic Acid (PLA) materials [Master's thesis]. Halmstad University: Sweden.
46. Durán Redondo D (2019) Circular economy through plastic recycling process into 3D printed products: A frugal solution for schools [Master's thesis]. Universitat Politècnica de Catalunya: Spain.

AIMS Press